Fluctuation effects at the free surface of superfluid ^{4}He

2000 J. Phys.: Condens. Matter 12 6009

(http://iopscience.iop.org/0953-8984/12/28/301)

J. Phys.: Condens. Matter **12** (2000) 6009–6022. Printed in the UK PII: S0953-8984(00)13188-1

Fluctuation effects at the free surface of superfluid ^{4}He

D E Galli† and L Reatto

INFM and Dipartimento di Fisica, Università degli Studi di Milano, Via Celoria 16, 20133 Milano, Italy

Received 12 April 2000

Abstract. We report our results about the fluctuation effects on the surface static structure factor and on the local Bose–Einstein condensate (BEC) in the low density surface region of ^{4}He. This information has been obtained by a variational Monte Carlo calculation for a slab of ^{4}He modelled by a novel shadow wave function with a glue term (glue-SWF). This glue-SWF describes the self-binding of ^{4}He only via local interparticle correlations. BEC increases from the bulk-like value well inside the slab to a much larger value in the surface region (up to about 50%). Further out of the surface the condensate decreases and correspondingly there is an enhanced population of small momentum states. This is very different from the full BEC that was predicted using a simplified variational treatment of these ^{4}He systems. This different behaviour is correlated with the presence in the glue-SWF of enhanced density fluctuations in the surface region as shown by the behaviour of the static structure factor at small wave vector. This is interpreted as an effect due to the zero point motion of ripplons.

1. Introduction

The treatment of highly inhomogeneous states of a quantum fluid such as ^{4}He has attracted much attention and methods developed for the uniform case have been extended to treat cases like a cluster, a film on a solid substrate or the liquid–vacuum interface. The inhomogeneity has two different origins. In the case of a thin film like a monolayer or a bilayer on a substrate it is the binding to the substrate, usually much stronger than the interatomic binding, which is controlling, to a large extent, the inhomogeneity. Such inhomogeneity would be present also in the hypothetical case of a fluid made of particles with just repulsive interatomic forces, as in the case of hard spheres. The situation is different in the case of a cluster or of the free surface of a fluid. Here the inhomogeneity arises because the system possesses a bound state so that under certain circumstances the system lowers its energy by forming interfaces and not by filling in a uniform way all the allowed space. The current theoretical treatments do not stress such a difference and all inhomogeneities are treated essentially in the same way. Here we show that a novel way to represent self-binding in a quantum system introduced few years ago [1] is successful from the energetic point of view but it gives a very different and more realistic picture compared with the standard treatment for surface fluctuations related aspects. Recently [2] it has been suggested that the low density surface region of ^{4}He is a physical system that possesses full Bose–Einstein condensation (BEC). But BEC is a fragile effect that may easily be affected by other properties of the system. For instance, from our calculations we find that the local BEC does not reach full condensation in the low density surface region as found with standard wave functions (wf) but actually there is first an increase of BEC in the

† To whom correspondence should be addressed.

0953-8984/00/286009+14$30.00

surface region due to the lowering of the local density followed by a strong depression due to surface fluctuations.

2. Self-binding with glue-SWF

Here we only consider the case of bosons at $T = 0$ K and ^{4}He is the physical system we have in mind. The standard theoretical treatment is based on the variational approach and the inhomogeneity is induced in the system by the presence of Hartree-like terms, i.e. by single particle factors, in the ground state wf Ψ_0. The simplest approximation for a strongly interacting system like ^{4}He is the Hartree–Jastrow form, in which interparticle correlations are represented by pair terms so that Ψ_0 reads

$$\Psi_0(R) = \prod_i f^{(1)}(\vec{r}_i) \prod_{l<m} f^{(2)}(r_{lm}). \tag{1}$$

$R = \{\vec{r}_1, .., \vec{r}_N\}$ represent the coordinates of the N bosons and $f^{(1)}$ and $f^{(2)}$ are non-negative functions which are determined by minimization of the expectation value of the Hamiltonian. It is recognized [3] that the pair term $f^{(2)}$ should depend separately on $\vec{r}_l$ and $\vec{r}_m$, but in the actual computations one usually assumes a bulk-like form, i.e. a dependence just on the pair distance $r_{lm} = |\vec{r}_l - \vec{r}_m|$. A better representation of Ψ_0 is obtained if (1) is supplemented by correlations between triplets of particles. No variational computation has been performed yet with the more general form, in which $f^{(2)}$ is assumed to depend separately on $\vec{r}_l$ and $\vec{r}_m$, presumably due to the difficulty of modelling such dependence. A different strategy is to include many-particle correlations in Ψ_0 via the technique of subsidiary variables, the so called shadow wf (SWF). This technique has given superior results [4], not only for the ground state but also for excited states, and we adopt it here by a suitable extension which is able to represent self-binding.

Binding in a quantum system at $T = 0$ K is peculiar because the dense system coexists with a vacuum, not with a vapour as in a classical system. This means that the quantum probability density $P(R) = |\Psi_0(R)|^2$ cannot have a classical analogue with a system with local interparticle interactions. We noticed that the following form of Ψ_0 has the desired properties:

$$\Psi(R) = \int \mathrm{d}S F(R, S) \times L(S) \tag{2}$$

where $S = \{\vec{s}_1, .., \vec{s}_N\}$ are the coordinates of a set of subsidiary variables (shadows). $F(R, S)$ contains correlations between particles, between shadows and between particles and shadows of the pair form

$$F(R, S) = \phi_p(R) \times \prod_{i=1}^{N} f_{ps}(|\vec{r}_i - \vec{s}_i|) \times \phi_s(S). \tag{3}$$

$\phi_p(R) = \prod_{i<j=1}^{N} f_p(|\vec{r}_i - \vec{r}_j|)$ is a Jastrow factor, and similarly for $\phi_s(S) = \prod_{i<j=1}^{N} f_s(|\vec{s}_i - \vec{s}_j|)$. Integration over shadow coordinates implicitly introduces correlations between particles beyond the pair (Jastrow) level at all orders. The glue factor $L(S)$ has the form:

$$L(S) = \prod_{i=1}^{N} \exp\left[-D\frac{(\hat{n}_i - 1)^2}{\hat{n}_i}\right]. \tag{4}$$

$\hat{n}_i$ represents a suitably normalized local density operator of shadow variables around the i-th shadow:

$$\hat{n}_i = \frac{1}{A} \sum_{j(\neq i)} l(|\vec{s}_i - \vec{s}_j|) \qquad l(s) = \mathrm{e}^{-\mu s^2}. \tag{5}$$

The correlations introduced with the glue factor $L(S)$ act as a 'spring', trying to keep $\hat{n}_i$ not too far from 1. When the system is homogeneous the argument of the exponential function in $L(S)$ can be expanded around the average value $\langle \hat{n}_i \rangle$ of the local density operator. To the lowest order in $\hat{n}_i - \langle \hat{n}_i \rangle$ one can easily see that the effect of the glue factor $L(S)$ is simply that of renormalizing the Jastrow factor f_s for the shadow. To second order, it introduces triplet correlations between the shadow variables. If the fluctuations around $\langle \hat{n}_i \rangle$ are small then these effective couplings will be small too. The situation is very different should the homogeneous state be such that $\langle \hat{n}_i \rangle$ is much below unity. This is the case in which N atoms have a large volume V available so that $N/V << \rho_0$, where ρ_0 is the equilibrium density of the system. In this case the glue term causes a symmetry breaking in the state of the system, i.e. the N atoms do not fill uniformly the volume V, but only partially fill it, so that $\hat{n}_i$ stays close to unity. In other words we have a phase separation into a dense region and a remaining region. Actually this remaining region has zero density. In fact, the probability that a single particle can escape from the fluid is zero due to the presence of $\hat{n}_i$ in the denominator in the exponential of equation (4): a configuration in which one ^{4}He atom is far from the rest of the system causes $\hat{n}_i$ to be near zero and therefore also $L(S)$ so that the SWF vanishes. In principle we could have evaporation of dimers or trimers, but the actual computation shows that this never happens when the wf is optimized for ^{4}He. In this way we are able to reproduce the self-bound properties of ^{4}He in the presence of a free surface. For the correlating factors contained in $F(R, S)$ we assume that they are the same for bulk ^{4}He and we have used those which have been recently fully optimized [4] in the bulk liquid. The only new variational parameters are contained in $L(S)$. Specifically D, μ and A are the variational parameters which have been optimized in this calculation. D controls the force of the 'spring', μ characterizes the range of the local density operator and A controls the average density of the system.

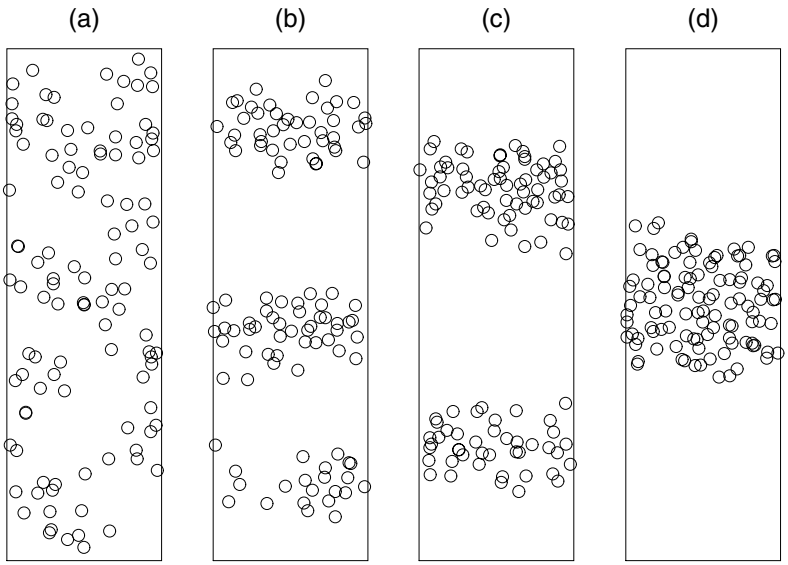

Figure 1. Projection of the positions of the particles on the x–z plane after a dilatation for a factor of five in the z-direction. The panels correspond to configurations after 250 (a), 7500 (b), 10^5 (c) and 2×10^5 (d) Monte Carlo steps.

In order to prove the self binding property of our wf we have performed the following computer experiment. We start the simulation with V and N with N/V of order of ρ_{eq} or above and in this way the particles fill the space uniformly, reproducing the bulk system. We have verified that the energy, the correlations and also the BEC fraction are essentially unaffected by the presence of the glue term $L(S)$. At a certain point of the simulation, the simulation box is expanded by a large factor. One can proceed in two ways. In the first, the positions of the particles and shadows are unchanged when the volume V is increased. In the second, one performs a dilatation also of the coordinates of particles and shadows when V is increased. After relaxation we find that the final state is the same irrespective of the way the dilatation is performed: the system is found to be in a dishomogeneous state forming either a droplet or a spanning slab across the volume V depending on the geometry of the box after dilatation. Let us stress that we have achieved with the glue-SWF self-binding only via local interparticle correlations. As an example, in figure 1 we show the evolution after the dilatation has been performed along only one of the sides of the initially cubic simulation box. At the same time the coordinates have also been expanded. The process of coalescence is clear. In this case since only one side of the simulation box has been expanded (the one in the z-direction) the preferred equilibrium geometry is a slab perpendicular to the z-axis. Should one expand the simulation box in all three directions the final state would be a cluster.

3. Ground-state results

With the glue-SWF we have studied both slabs of different thicknesses and droplets with different number of particles. The energetics and the density profile are similar to previous results obtained with standard variational techniques and these results compare favourably with exact quantum Monte Carlo methods. Figures 2 and 3 show, respectively, the density profile along the z-axis for slabs and the radial density profile for droplets calculated with the glue-SWF for different number of ^{4}He atoms.

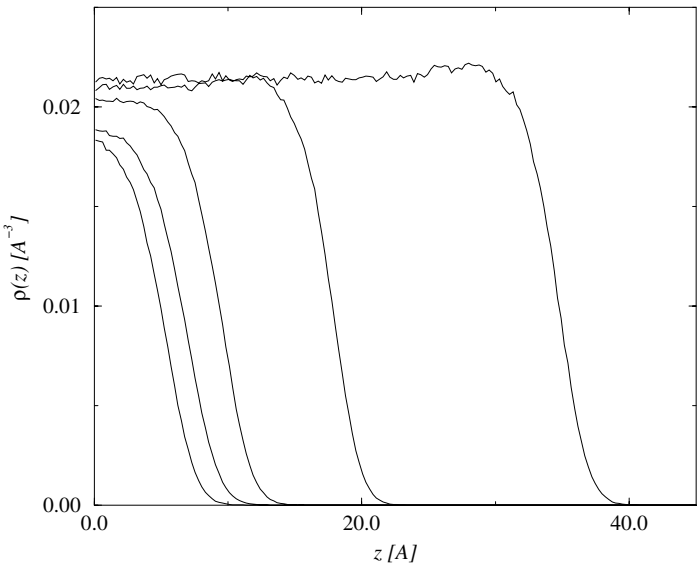

Figure 2. Density profile $\rho(z)$ of slabs with different number of particles ($N = 54, 72, 108, 216, 432$) as given by the glue-SWF. The slab is symmetric with respect to $z = 0$.

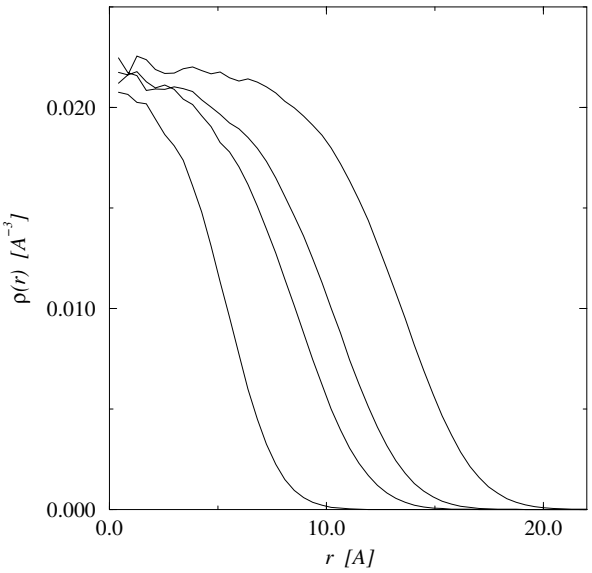

Figure 3. Radial density profile $\rho(r)$ for clusters with different number of particles ($N = 20, 70, 112, 240$).

In tables 1 and 2 we collect some of the properties obtained in the simulation of self-bound slabs and droplets with the glue-SWF; we compare our results with those found with the standard variational approach or with some exact quantum Monte Carlo methods such as the diffusion Monte Carlo (DMC) and the Green function Monte Carlo (GFMC). In our simulation the slabs have different numbers of particles but the surface area A is kept constant to the value $A = 290.6$ Å^2. From an energetic point of view, the description of a self-bound state with the glue-SWF is successful; we obtain results that are similar to the energies found with the other techniques. A first sign of the differences that one finds in the description of the surface properties of an ^{4}He system with the glue-SWF can be seen in the greater surface width W that we obtain.

Table 1. Properties of ^4He_N slabs. $\langle E\rangle/N$ is the total energy per particle of the slab. W is the width of the surface ($0.9\rho \rightarrow 0.1\rho$). D, μ and A are the variational parameters obtained in the optimization of the glue factor in equation (4). In order to comply with the periodic boundary conditions the function $l(s) + l(L - s) - 2l(L/2)$ in place of $l(s)$ has been used, where L is the side of the simulation box parallel to the surface.

Method	N	$\langle E\rangle/N$ [K]	$\sqrt{\langle z^2\rangle}$[Å]	W[Å]	D	μ [Å^{-2}]	A
SWF	54	-4.06 ± 0.03	3.47 ± 0.31	5.06	0.35	1.53×10^{-2}	3.9
SWF	72	-4.67 ± 0.03	4.41 ± 0.48	5.52	0.35	1.53×10^{-2}	3.8
SWF	108	-5.38 ± 0.03	5.65 ± 0.53	5.26	0.30	1.53×10^{-2}	5.3
SWF	216	-6.13 ± 0.02	10.33 ± 0.94	4.75	0.35	1.53×10^{-2}	5.7
SWF	432	-6.52 ± 0.02	20.06 ± 1.8	4.8	0.25	1.53×10^{-2}	8.0
VMC [5]	54	-4.06 ± 0.03	3.48	3.1	–	–	–
VMC [5]	108	-5.31 ± 0.03	5.84	3.5	–	–	–
VMC [5]	216	-5.98 ± 0.03	10.28	4.3	–	–	–
GFMC [5]	54	-4.65 ± 0.03	3.47	3.1	–	–	–
GFMC [5]	108	-5.69 ± 0.03	5.86	3.7	–	–	–

Table 2. Properties of ^4He_N droplets. $\langle E\rangle/N$ is the total energy per particle of the cluster. r_0 is defined as $r_0 = (5/3)^{1/2}\langle r^2\rangle^{1/2}N^{-1/3}$ and W is the width of the surface $(0.9\rho \rightarrow 0.1\rho)$. D, μ and A are the variational parameters obtained in the optimization of the glue factor in equation (4).

Method	N	$\langle E\rangle/N[K]$	r_0[Å]	W[Å]	D	μ [Å^{-2}]	A
SWF	20	-1.52 ± 0.03	2.71	5.11	0.45	1.53×10^{-2}	19.9
SWF	70	-2.93 ± 0.02	2.47	7.05	0.35	1.53×10^{-2}	32.0
SWF	112	-3.40 ± 0.02	2.55	8.07	0.35	1.53×10^{-2}	36.6
SWF	240	-4.14 ± 0.02	2.46	7.8	0.30	1.53×10^{-2}	53.0
VMC [6]	20	-1.51	2.73	5.4	–	–	–
VMC [6]	70	-3.0	2.42	3.5	–	–	–
VMC [6]	112	-3.5	–	–	–	–	–
VMC [6]	240	-4.19	2.36	4.1	–	–	–
DMC [7]	20	-1.66	2.68	–	–	–	–
DMC [7]	70	-3.2	2.43	–	–	–	–
DMC [7]	112	-3.73	2.42	–	–	–	–
GFMC [8]	20	-1.63	–	–	–	–	–
GFMC [8]	70	-3.12	–	–	–	–	–
GFMC [8]	112	-3.6	–	–	–	–	–

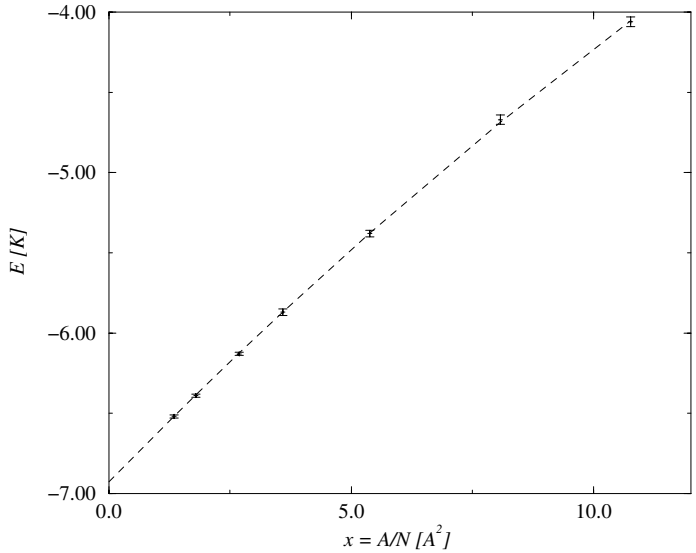

Figure 4. Energies per particle for slabs with different thickness versus $x = A/N$. The curve is the second-degree polynomial fit to our results.

As shown in [5], from simulation of slabs with different thicknesses and different number of atoms N but with a constant surface area A, one can extract the bulk energy E_{bulk}, the surface energy and higher order terms. If we define $x = A/N$ one has $E(N)/N = E_{bulk}+\sigma x+\delta x^2+\ldots$ where σ is the surface tension. In figure 4 we plot E as function of x for slabs with different thicknesses ($N = 54$, 72, 108, 162, 216, 324, 432) and the parabola which fits our results. From the fit we find $E_{bulk} = -6.929 \pm 0.021$ K, $\sigma = 0.31 \pm 0.01$ K Å^{-2} and $\delta = -0.0040\pm0.0009$. E_{bulk} as given from the fit is in agreement with energy per particle found [4] in the simulations of the bulk liquid $E/N = -6.937 \pm 0.006$ K. Previous Green function and variational Monte Carlo methods [5] gave surface tensions of $\sigma = 0.265 \pm 0.006$ K Å^{-2}

and $\sigma = 0.272 \pm 0.011$ K Å^{-2}, respectively. Recent experimental results [9] have measured a surface tension of $\sigma = 0.272 \pm 0.002$ K Å^{-2}. Our result for σ is about 13% higher than these values.

4. Fluctuation properties of the interface

Starting from a successful variational description of a self-bound ^{4}He system, now we want to investigate the fluctuation properties of the interface and their influence on the local BEC at the free surface. The zero point motion of the low energy excitations in a quantum fluid determines the small k behaviour of the static structure factor. For instance, the zero point motion of phonons in bulk ^{4}He gives the characteristic behaviour $S(k) = \hbar k/2mc$ at small k where c is the sound velocity. In ^{4}He with a free surface in addition to phonons, another branch of excitations appears, the ripplons. It is known that these excitations, which are surface modes, propagate close to the liquid–vacuum interface with energy given by the dispersion relation

$$\varepsilon_r\left(k_\parallel\right) = \hbar\sqrt{\frac{\sigma}{m\rho_{eq}}}k_\parallel^{3/2}. \tag{6}$$

$\vec{k}_\parallel$ is the wave vector parallel to the surface, σ the surface tension and ρ_{eq} the density well inside the liquid. Let us define a z-dependent structure factor

$$S\left(k_\parallel, z, z'\right) = \frac{A^{-2}}{\rho(z)\rho(z')}\left\langle \sum_m \mathrm{e}^{i\vec{k}_\parallel\cdot\vec{r}_m}\delta\left(\vec{r}_m\cdot\hat{\vec{j}} - z\right)\sum_\ell \mathrm{e}^{i\vec{k}_\parallel\cdot\vec{r}_\ell}\delta\left(\vec{r}_\ell\cdot\hat{\vec{j}} - z'\right)\right\rangle \tag{7}$$

where $\hat{\vec{j}}$ is the unit vector in the z-direction normal to the surface and A is the cross section of the slab. $S(k_\parallel, z, z')$ measures the density fluctuations of wave vector $k_\parallel$ between particles, one at height z and one at height z'. The diagonal part $S(k_\parallel, z, z)$ gives the static structure factor for particles within a layer characterized by the coordinate z. It has been shown [3] that the zero point motion of ripplon excitations at the free surface gives a contribution S_r to $S(k_\parallel, z, z')$, which at small $k_\parallel$ has the following behaviour:

$$S_r\left(k_\parallel, z, z'\right) \sim 2\sqrt{\frac{\hbar^2}{m\sigma\rho_{eq}}}\frac{\mathrm{d}\sqrt{\rho\,(z)}}{\mathrm{d}z}\frac{\mathrm{d}\sqrt{\rho\,(z')}}{\mathrm{d}z'}k_\parallel^{-1/2}. \tag{8}$$

The $k_\parallel^{-1/2}$ divergence at $k_\parallel = 0$ is a manifestation of large density fluctuations due to ripplons. Notice that these fluctuations are present only when z and z' are in the interfacial region where $\mathrm{d}\rho(z)/\mathrm{d}z$ is non-zero. As we move from the interface to the interior, the ripplon contribution S_r goes to zero and the $k_\parallel^{-1/2}$ divergence crosses over to the linear behaviour in $k_\parallel$ typical of the bulk so that $S(k_\parallel, z, z)$ does not diverge but vanishes at $k_\parallel = 0$.

We have computed the z-dependent structure factor (7) for a slab of ^{4}He described by a standard wf equation (1) and by the glue-SWF. The result for a standard wf with one-body terms and bulk-like pair terms are shown in figure 5.

In this case we do not find any enhancement of the density fluctuations in the surface region. $S(k_\parallel, z, z)$ smoothly goes to 1 both at small and at large $k_\parallel$. At first sight this seems reasonable. As z moves from the interior of the slab to the surface, the density decreases and $S(k_\parallel, z, z)$ evolves from a bulk-like behaviour to that of a very diluted system for which $S(k) = 1$. In contrast, in the case of the glue-SWF (see figure 6) $S(k_\parallel, z, z)$ becomes large at small $k_\parallel$ when z is such that $\mathrm{d}\rho(z)/\mathrm{d}z$ is large. Notice also the persistence of a peak in $S(k_\parallel, z, z)$ at large $k_\parallel$ even when the local density is almost two orders of magnitude smaller

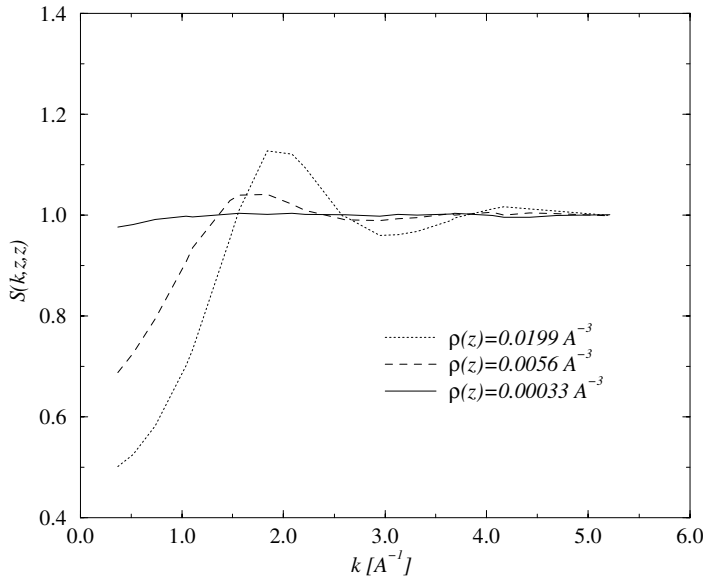

Figure 5. Static structure factor $S(k_\parallel, z, z)$ computed with a standard wf with one-body terms and bulk-like pair terms. $S(k_\parallel, z, z)$ is shown for three different values of z such that the local density assumes the values in the legend.

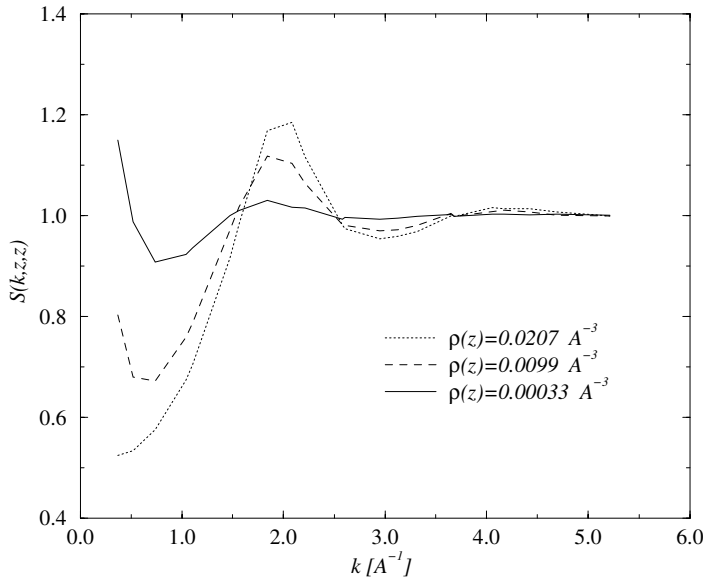

Figure 6. Static structure factor $S(k_\parallel, z, z)$ computed with a glue-SWF. $S(k_\parallel, z, z)$ is shown for three different values of z such that the local density assumes the values in the legend.

than the bulk density. This means that even in the tail of the density profile the particles are strongly correlated. At the same time the large value of $S(k_\parallel, z, z)$ at small $k_\parallel$ indicates the presence of a strong clustering tendency.

We can get a physical picture of this. Consider a surface wave on a planar surface. A large amplitude wave is perhaps not very frequent, but when it takes place a particle on the top of the wave is surrounded by other particles because the local density is high even if the *average* density is small. This is true even at $T = 0$ K where a real ripplon excitation is replaced by its zero point motion. We can easily see this effect just by analysing the configurations along the Monte Carlo run as in figure 1. We conclude that in a self-bound system the presence of a region of very low density is not so much due to single particle penetrations of a potential barrier (that due to the self-consistent field due to the other atoms) but to a collective effect. We can substantiate this picture by comparing our $S(k_\parallel, z, z')$ with the one (equation (8)) given by the ripplon theory. In order to distinguish the collective contribution to $S(k_\parallel, z, z')$ we take the difference between the $S(k_\parallel, z, z')$ computed with the glue-SWF and the same static structure factor computed with the standard variational approach. This difference turns out to be in quantitative agreement (see figure 7) with the ripplon contribution obtained from the formula (8) in which we use for σ and $\rho\,(z)$ the values given by the glue-SWF.

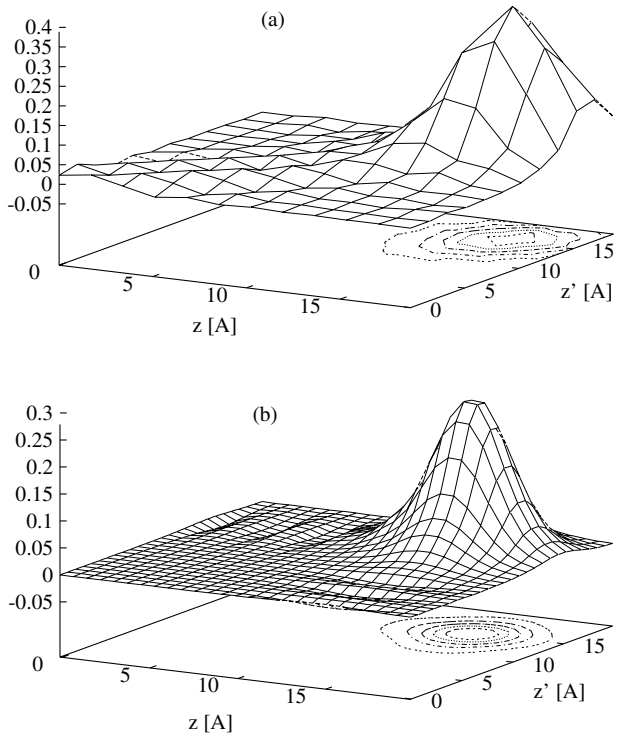

Figure 7. (a) Difference between the two $S(k_\parallel, z, z')$ computed from the glue-SWF and from the standard variational wf as function of z and z' (only $z, z' > 0$ are shown). (b) $S(k_\parallel, z, z')$ from equation (8). In (a) and in (b) $k_\parallel \simeq 0.37$ Å^{-1} (this is the smallest $k_\parallel$ allowed by our simulation cell).

We conclude that the glue-SWF contains the basic phenomenon of ripplon fluctuations whereas the standard wf does not. Notice that in our computation there is a lower cut-off to $k_\parallel$ due to the finite size of the system, so that we cannot describe the $k_\parallel^{-1/2}$ singularity but only the enhancement of the density fluctuations at small but finite $k_\parallel$. In addition, to recover the

$k_\parallel^{-1/2}$ singularity the pseudopotentials should have a suitable long range contribution which is absent in the present parametrization of the glue-SWF.

In order to study the size dependence of $S(k_\parallel, z, z)$ we have performed some computation for a larger number of particles as well as with an increased area A of the slab. For a given $k_\parallel$ we find that this size dependence is small, below the noise level of the simulation. On the other hand with a larger value of A one has access to smaller values of $k_\parallel$ and we find that $S(k_\parallel, z, z)$ given by the glue-SWF continues to increase as $k_\parallel$ becomes smaller, as one would expect on the basis of equation (8).

5. Bose–Einstein condensation and momentum distribution

In a slab geometry also the momentum distribution for $\vec{k}$ parallel to the surface has a well defined meaning and one can consider a z-dependent momentum distribution $n(k_\parallel, z)$. Of special interest is the Bose–Einstein condensate fraction $n_0(z)$, i.e. the fraction of particles with $k_\parallel = 0$, as function of z. In order to study the local condensate fraction we have computed the one-body density matrix [11] and analysed its off-diagonal long range order. The one-body density matrix is given by

$$\rho_1(\vec{r}, \vec{r}') = N \int \mathrm{d}\vec{r}_2 \ldots \mathrm{d}\vec{r}_N \Psi(\vec{r}, \vec{r}_2, \ldots, \vec{r}_N)\Psi(\vec{r}', \vec{r}_2, \ldots, \vec{r}_N). \tag{9}$$

In the slab geometry the one-body density matrix is a function of the z components of $\vec{r}$ and $\vec{r}'$ and of R_{xy}, the modulus of the projection of $\vec{r} - \vec{r}'$ on the x–y plane: $\rho_1(\vec{r}, \vec{r}') = \rho_1(R_{xy}, z, z')$ where $R_{xy} = \sqrt{(x - x')^2 + (y - y')^2}$. As shown by Krotscheck [12], when R_{xy} goes to infinity, the one-body density matrix converges to

$$\lim_{R_{xy}\to\infty} \rho_1(R_{xy}, z, z') = \left[\rho(z)\rho(z')n_0(z)n_0(z')\right]^{\frac{1}{2}} \tag{10}$$

where $\rho(z)$ is again the density profile of the slab and $n_0(z)$ is the local condensate fraction at height z. Therefore, from $\rho_1(R_{xy}, z, z)$ we can extract the condensate fraction by analysing the long range limit

$$\lim_{R_{xy}\to\infty} \frac{\rho_1(R_{xy}, z, z)}{\rho(z)} = n_0(z). \tag{11}$$

We have computed ρ_1 first with a standard wf and the results are shown in figure 8. Our result agrees with previous results: a standard wf with one-body and bulk-like Jastrow terms gives $n_0(z)$, which is a smoothly increasing function as one moves from the middle of the slab to the tail region of the surface where the density becomes small. In the middle of the slab ($z \sim 0$ Å), where the density is near the equilibrium value, the local condensate is about 10% (the value found in bulk ^{4}He). Upon approaching the surface n_0 increases; for instance it is 70% when $\rho(z)$ is about 10% of ρ_{eq} and it reaches full condensation when $\rho(z)$ is of order or below 1% of ρ_{eq}.

A quite different result is found with the glue-SWF as it is shown in figure 9: in the middle of the slab we find the usual bulk-value for the local condensate. Upon approaching the interfacial region first $n_0(z)$ rapidly rises up to about 50% when $\rho(z)$ is about 10% of ρ_{eq}, but further out in the tail region $n_0(z)$ decreases to small values. Actually in this region we are able to give only an upper bound for the condensate fraction because the long range limit of $\rho_1(R_{xy}, z, z)$ is not reached within the maximum distance allowed by the simulation box (see figure 9). In figure 10 we show n_0, as obtained by the long range limit of $\rho_1(R_{xy}, z, z)$, computed with the standard wf and with the glue-SWF, and plotted as function of the local density of the slab. By comparing ρ_1 with $S(k_\parallel, z, z)$ we find that the depletion of the condensate in the surface

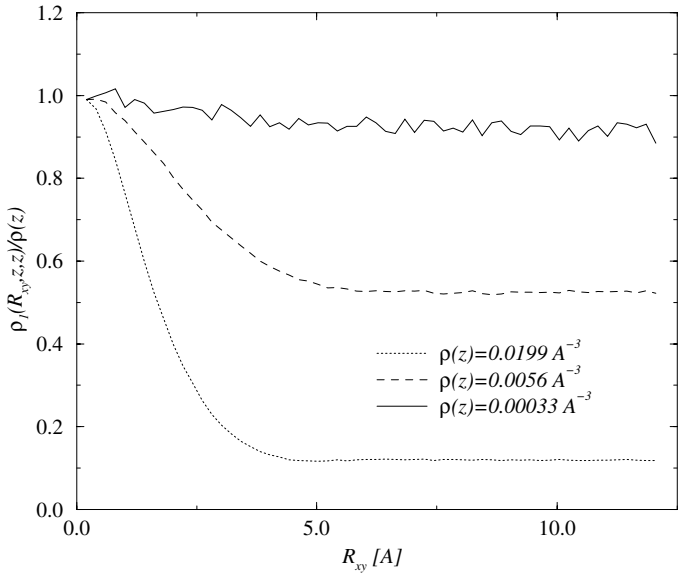

Figure 8. $\rho_1(R_{xy}, z, z)/\rho(z)$ as computed with a standard wf with one-body and bulk-like Jastrow terms for three different distances from the surface where the density assumes the values in the legend.

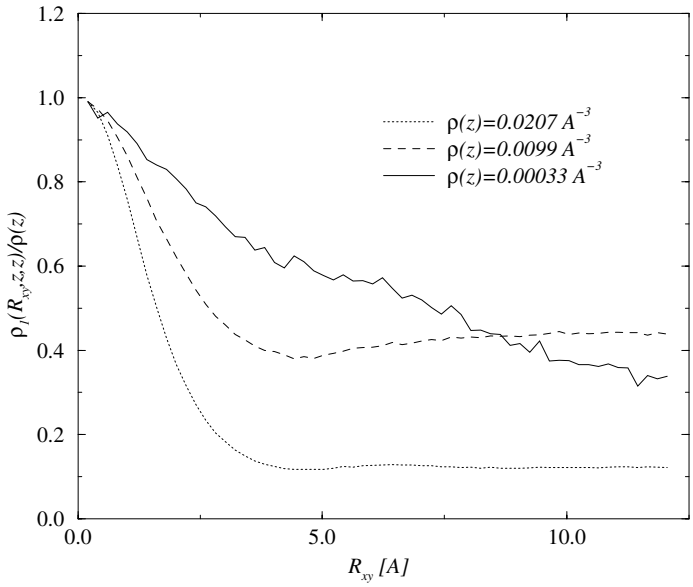

Figure 9. $\rho_1(R_{xy}, z, z)/\rho(z)$ as computed with a glue-SWF for three different distances from the surface where the density assumes the values in the legend.

region starts to take place where the ripplon enhancement of $S(k_\parallel, z, z)$ is maximum. This result indicates that ripplon fluctuations have a strong depletion effect on the local condensate fraction at the free surface. The quantum state that one obtains by displacing a particle in the

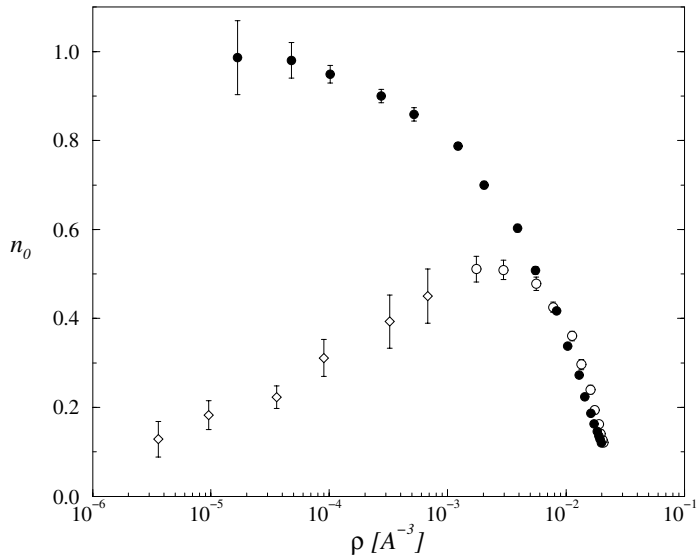

Figure 10. n_0 as function of the value of the local density of the slab for a standard wf (filled circles) and for the glue-SWF (open symbols). In the low density region diamonds represent only an upper bound for the condensate fraction because the long range limit of $\rho_1(R_{xy}, z, z)$ is not reached within the maximum distance allowed by the simulation box.

surface region to a large distance parallel to the surface has still a finite overlap with the original quantum state, but due to the presence of the zero-point motion of ripplons, this overlap is strongly depressed even if the local density is very small and the system would appear as weakly interacting. We find also that in correspondence of the depletion of the condensate in the tail region of the surface there is an associated promotion of particles at small momenta. We see this effect by computing a z-dependent momentum distribution $n(k_\parallel, z)$, i.e. the momentum distribution for $\vec{k}$ parallel to the surface. This function is related to $\rho_1(R_{xy}, z, z)$ simply via a two dimensional Fourier transform. In figure 11 we show the results for the computation of $n(k_\parallel, z)$. The three curves correspond to the same regions of the slab for which we have shown the static structure factor in figure 6.

An interesting problem is how the momentum distribution depends on the size of the system. We have not been able to study this because the computation of the one-body density matrix is very heavy and presently we are not able to increase in an appreciable way the number of particles. The present results have been obtained for a slab with $N = 162$ ^{4}He atoms and a surface area of $A = 290.6$ Å^2.

The interpretation of the SWF results is rather direct in terms of two competing effects on the local condensate. The decreasing value of the local density as the surface is approached causes an enhancement of $n_0(z)$ because the system is less strongly interacting. This effect is contrasted by ripplon effects. As discussed above, when the local density becomes rather small this small value of $\rho(z)$ is due more to the presence of ridges and valleys due to the zero point motion of ripplons than to single particle penetration of a barrier. This means that when we destroy a particle at the x–y plane this particle comes most likely from a locally dense region, from the ridge of a wave (figure 12). As we transfer this particle at some distance R_{xy} by keeping the same value of z this particle will be floating on the average at some distance from a valley of the wave but for such configuration the wf will be small due to the glue term. This

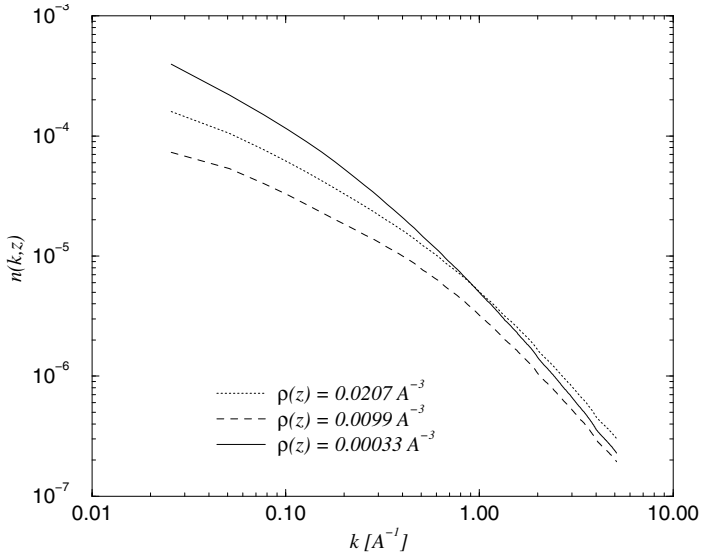

Figure 11. Momentum distribution $n(k_\parallel, z)$ for wave vector $\vec{k}$ parallel to the surface as obtained from the glue-SWF. Notice the logarithmic scale.

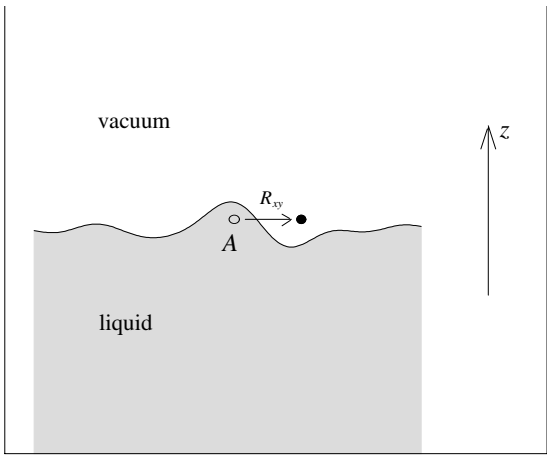

Figure 12. Representation of the process in which a particle is destroyed in position A and it is transferred a distance R_{xy} apart.

means that $\rho_1(R_{xy}, z, z)$ will be depressed for large R_{xy} so that also $n_0(z)$ decreases. No such effect is present with the standard wf because the only z-dependent terms are the one-body ones.

It is also interesting to look at the behaviour of $n(k_\parallel, z)$. On going from the middle of the slab to the surface region where there is an enhancement of particles in the zero-momentum state one finds a depression of $n(k_\parallel, z)$ at all finite $k_\parallel$. This trend is reversed further out in the surface where the zero-point motion of ripplons induces a depletion of the condensate fraction: due to small $k_\parallel$ fluctuations there is a large promotion of particles at small momentum. We have studied the local condensate also in the case of clusters and we find rather similar results.

6. Conclusion

We conclude that the zero point motion of ripplon fluctuations has a strong effect on some of the ground state properties of the free surface of liquid ^{4}He. These effects are manifested especially in the local condensate fraction and in the local momentum distribution. Unfortunately, these quantities are not easily measurable experimentally. The other quantity which is strongly affected by ripplons is the static structure factor $S(k_\parallel, z, z)$ in the surface region, for which we predict a well-defined signature of fluctuations: a large value of $S(k_\parallel, z, z)$ at small $k_\parallel$ and the persistence of short range correlations even when the local density is very small. Measurement of $S(k_\parallel, z, z)$ should be feasible by performing diffraction measurements under total reflection conditions. All these results indicate that the tail region of the liquid–vacuum interface is very different from a rarefied system.

Acknowledgments

This work was supported by the INFM Parallel Computing Initiative.

References

[1] Galli D E and Reatto L 1996 *Monte Carlo and Molecular Dynamics of Condensed Matter Systems*, ed K Binder and G Ciccotti (Bologna: SIF)
[2] Griffin A and Stringari S 1996 *Phys. Rev. Lett.* **76** 259
[3] Krotscheck E, Stringari S and Treiner J 1987 *Phys. Rev.* B **35** 4754
[4] Moroni S, Galli D E, Fantoni S and Reatto L 1998 *Phys. Rev.* B **58** 909
[5] Valles J L and Schmidt K E 1988 *Phys. Rev.* B **38** 2879
[6] Pandharipande V R, Pieper S C and Wiringa R B 1986 *Phys. Rev.* B **34**, 4571
[7] Chin S A and Krotscheck E 1992 *Phys. Rev.* B **45** 852
[8] Pieper S C, Wiringa R B and Pandharipande V R 1985 *Phys. Rev.* B **32** 3341
[9] Deville G, Roche P, Appleyard N J and Williams F I B 1996 *Czech. J. Phys.* **46** (S1) 89
[10] Lewart D S, Pandharipande V R, Pieper S C 1988 *Phys. Rev.* B **37** 4950
[11] Penrose O and Onsager L 1956 *Phys. Rev.* **104** 576
Campbell C E 1993 *J. Low Temp. Phys.* **93** 907
[12] Krotscheck E 1985 *Phys. Rev.* B **32** 5713